

Isosteviol Sodium Protects Neural Cells Against Hypoxia-Induced Apoptosis Through Inhibiting MAPK and NF-κB Pathways

Kai-Lun Zhong, MD,¹ Min-Yi Lu, MD,¹ Fei Liu, MD, Ying Mei, MD, Xue-Ju Zhang, PhD, Hao Zhang, PhD, Jie Zan, PhD, Xiao-Ou Sun, PhD, and Wen Tan, PhD

Background: Stevioside, isolated from the herb *Stevia rebaudiana*, has been widely used as a food sweetener all over the world. Isosteviol Sodium (STV-Na), an injectable formulation of isosteviol sodium salt, has been proved to possess much greater solubility and bioavailability and exhibit protective effects against cerebral ischemia injury in vivo by inhibiting neuron apoptosis. However, the underlying mechanisms of the neuroprotective effects STV-Na are still not completely known. In the present study, we investigated the effects of STV-Na on neuronal cell death caused by hypoxia in vitro and its underlying mechanisms. **Methods:** We used cobalt chloride (CoCl₂) to expose mouse neuroblastoma N2a cells to hypoxic conditions in vitro. **Results:** Our results showed that pretreatment with STV-Na (20 μM) significantly attenuated the decrease of cell viability, lactate dehydrogenase release and cell apoptosis under conditions of CoCl₂-induced hypoxia. Meanwhile, STV-Na pretreatment significantly attenuated the upregulation of intracellular Ca²⁺ concentration and reactive oxygen species production, and inhibited mitochondrial depolarization in N2a cells under conditions of CoCl₂-induced hypoxia. Furthermore, STV-Na pretreatment significantly downregulated expressions of nitric oxide synthase, interleukin-1β, tumor necrosis factor-α, interleukin-6, nuclear factor kappa B (NF-κB), and mitogen-activated protein kinase (MAPK) signalings in N2a cells under conditions of CoCl₂-induced hypoxia. **Conclusions:** Taken together, STV-Na protects neural cells against hypoxia-induced apoptosis through inhibiting MAPK and NF-κB pathways.

Key Words: Cerebral ischemia—STV-Na—cobalt chloride—hypoxia—cell apoptosis—mitogen-activated protein kinase

© 2018 Published by Elsevier Inc. on behalf of National Stroke Association.

Introduction

Cerebral ischemia is one of the leading causes of adult mortality and disability and seriously threatens to human

health all over the world,¹⁻³ Numerous studies indicate that cerebral ischemia is a very complicated process with multiple mechanisms, including oxidative stress, excitotoxicity, mitochondrial dysfunction, intracellular

From the Institute of Biomedical and Pharmaceutical Sciences, Guangdong University of Technology, Guangzhou, China.

Received July 4, 2018; revision received September 11, 2018; accepted September 15, 2018.

This study was supported by the 2017 PhD Start-up Fund of Natural Science Foundation of Guangdong Province of China (2017A030310404), China Postdoctoral Science Foundation (Nos. 2017M622642 and 2017M622645) and Science and Technology Planning Project of Guangdong Province (No. 2015B010109004).

Address correspondence to Wen Tan, PhD, Institute of Biomedical and Pharmaceutical sciences, Guangdong University of Technology, Guangzhou 510006, China. E-mail: went@gdut.edu.cn

¹These authors equally contribute to this paper.

1052-3057/\$ - see front matter

© 2018 Published by Elsevier Inc. on behalf of National Stroke Association.

<https://doi.org/10.1016/j.jstrokecerebrovasdis.2018.09.020>

calcium overload, and apoptosis.⁴⁻⁶ Recently, a body of researches report that inflammation plays a critical role in cerebral ischemic damage.⁷⁻⁹ Cerebral ischemia activates inflammatory responses and produces cytotoxic substances including inducible nitric oxide synthase (iNOS), interleukin-1 β (IL-1 β), tumor necrosis factor- α (TNF- α), interleukin-6 (IL-6), and other proinflammatory mediators, eventually resulting in more neuronal death.¹⁰ A mount of studies have shown that nuclear factor kappa B (NF- κ B) and mitogen-activated protein kinase (MAPK) signaling cascades, including the extracellular signal-regulated kinases (ERK1/2), c-Jun NH2-terminal kinases (JNK), and p38, are activated in response to cerebral ischemia and play crucial roles in regulating proinflammatory mediators production, and apoptosis.¹¹⁻¹³ During ischemia, NF- κ B subunit p65 is activated by phosphorylation, translocates into the nucleus and then binds to the DNA binding site related to regulating the transcriptions of proinflammatory mediators genes.^{14,15} Moreover, MAPKs activation could also further activate transcription factors, inducing exaggerated synthesis of proinflammatory cytokines, subsequently triggering inflammatory responses, and institution of the apoptotic cascade.¹⁶ Nowadays, numerous studies show that natural products display neuroprotective effects by suppressing the NF- κ B and MAPK signaling pathways.¹⁷⁻¹⁹

Stevioside, a natural sweetener isolated from the herb *Stevia rebaudiana*, has been widely used as a food sweetener all over the world. Stevioside has been known to have a variety of properties including antihyperglycemic, antihypertensive, and anticancer.²⁰⁻²² STV-Na, an injectable formulation of isosteviol sodium salt, has been proved to possess much greater solubility and bioavailability and has the potential to be widely applied as an emergency treatment.²³ Recent studies reported that STV-Na exhibits protective effects against traumatic brain injury and permanent cerebral ischemia injury in vivo by inhibiting inflammatory responses²⁴⁻²⁶; however, the underlying mechanisms of the neuroprotective effects STV-Na on ischemia injury are still not completely known.

In the present study, we investigated the neuroprotective effects STV-Na using an in vitro ischemia model (mouse neuroblastoma N2a cells treated with cobalt chloride [CoCl₂]), which is a well-known hypoxia mimetic and has been widely used to mimic ischemic conditions in various cultured cells²⁷⁻²⁹ and its underlying mechanism. Our results demonstrate that STV-Na protects neuron cells from CoCl₂-induced hypoxia by attenuating expression of inflammatory factors via inhibiting the MAPKs and NF- κ B signaling pathways.

Materials and Methods

Cells and Reagents

Mouse neuroblastoma N2a cells, obtained from American Tissue Culture Collection (ATCC), were cultured in Dulbecco's modified Eagle's medium supplemented with 10% fetal

bovine serum, Penicillin/Streptomycin at 37°C in 5% CO₂. STV-Na was provided by the Chemical Development Laboratories of Key Biological Pharmaceutical Company (Dongguan, China). Cobalt chloride (CoCl₂) was purchased from Sigma Chemical Corporation.

Cell Viability Assay

Cell viability was measured using the Cell Counting Kit-8 (Beyotime, China), according to the manufacturer's instructions. Briefly, N2a cells were plated in 96-well plates and then treated with CoCl₂ alone. Some cells were pretreated with different concentrations of STV-Na 2 hours before CoCl₂ exposure. After the treatments, 10 μ l CCK-8 was added to each well, incubated for 2 hours at 37°C, and then the absorbance was measured at 450 nm using automated ELISA reader (47-1001, BERTHOLD TECHNOLOGIES, Germany). Cell viability was expressed as a percentage of the control.

Lactate Dehydrogenase Release Assay

The amount of lactate dehydrogenase (LDH) released from the cells at 24 hours after treatments was measured by the LDH Cytotoxicity Assay Kit (Beyotime, China), according to the manufacturer's instructions. Result of LDH release was expressed as a percentage of the control.

Flow Cytometric Analysis

Cell apoptosis was measured using the Annexin V-FITC/PI apoptosis kit (MultiScience, China), according to the manufacturer's instructions. Briefly, N2a cells cultured in 6-well plates were treated with CoCl₂ and/or STV-Na for 24 hours. The cells were harvested, washed twice with ice-cold Phosphate Buffered Saline (PBS), and then stained with 5 μ l Fluorescein isothiocyanate (FITC)-labeled Annexin-V and 10 μ l PI for 20 minutes at room temperature. Then, the stained cells were analyzed by flow cytometry (FACSCelesta 2, BD Biosciences, Franklin Lakes, NJ). The apoptotic rate was calculated as the percentage of early/primary apoptotic cells (Annexin V+/PI-) and late/secondary apoptotic cells (Annexin V+/PI+).

Determination of Intracellular Ca²⁺ of N2a Cells

The intracellular Ca²⁺ levels were determined using a fluorescence dye Fluo-4 AM (Beyotime, China), according to the manufacturer's instructions. Cells were washed with PBS twice and then loaded with 10 mmol/l Fluo-4 AM and 5 μ g/ml Hoechst 33342 for 30 minutes in incubator at 37°C in the dark. After that, the fluorescence of Ca²⁺ in cells was observed under a fluorescence microscope (Axio Image A2, Zeiss, Germany). The fluorescence intensity of Ca²⁺ was analyzed by Image J software.

Determination of Intracellular Reactive Oxygen Species of N2a Cells

The intracellular reactive oxygen species (ROS) levels were determined using an ROS Assay Kit (Beyotime, China), according to the manufacturer's instructions. Cells were washed with PBS twice and then loaded with 10 mmol/l DCFH-DA and 5 $\mu\text{g}/\text{ml}$ Hoechst 33342 for 30 minutes in incubator at 37°C in the dark. After that, the fluorescence of ROS in cells was observed under a fluorescence microscope (Axio Image A2, Zeiss, Germany). The fluorescence intensity of ROS was analyzed by Image J software.

Determination of Mitochondrial Membrane Potential of N2a Cells

The mitochondrial membrane potential (MMP) of N2a cells was determined using JC-1 dye (Beyotime, China), according to the manufacturer's instructions. Cells were washed with PBS twice and then stained with 2 $\mu\text{M}/\text{l}$ JC-1 at 37°C for 15 minutes. After that, JC-1 fluorescence was detected with confocal laser scanning microscopy (LSM800, Zeiss, Germany). Under the confocal laser scanning microscope, green fluorescence showed the cells with low $\Delta\Psi\text{m}$ indicating that JC-1 maintains monomeric form while red fluorescence showed the cells with high $\Delta\Psi\text{m}$. The relative proportions of red and green fluorescence were used to measure the extent of mitochondrial depolarization.

Quantitative Real-Time Polymerase Chain Reaction

The proinflammatory gene expression levels in cells were analyzed by quantitative real-time polymerase chain reaction (qRT-PCR), as previously described.²⁵ qRT-PCR primers were as follows: IL-6, 5'-GATT TACATAAAAATAGTCCTTCCTACC-3' and 5'-GGTTG CCGAGTAGATCTCAAAGTG-3'; TNF- α , 5'- α CAA GCCTGTAGCCCACGTC-3' and 5'- α AGACTCCTCCC AGGTATATGG-3'; IL-1 β , 5'- α CGATGCACCTGTA CGATCA-3' and 5'-TCTTTCAACACGCAGGACAG-3'; iNOS, 5'-GTTCTCAGCCCAACAATACAAGA-3' and 5'-GTGGACGGGTCGATGTCAC-3'; GAPDH, 5'-TC AACAGCAACTCCCCTCTTCCA-3' and 5'- α CCCTG TTGCTGTAGCCGTATTCA-3'.

Western Blotting

After treatment, N2a cells were collected and then lysed with NP40 lysis buffer (Beyotime, China). Whole cell lysates were subjected to Sodium dodecyl sulfate-polyacrylamide gel electrophoresis (SDS-PAGE) and immunoblotting, as previously described.²⁵ Primary antibodies against Bcl2 (ab32124, Abcam), Bax (ab32503, Abcam), cleaved caspase3 (ab49822, Abcam), p38 (14064-1 AP, Proteintech), phosphorylated p38 (p-p38) (ab47363, Abcam), JNK (51151-1 AP, Proteintech), phosphorylated

JNK (p-JNK; ab219584, Abcam), ERK1/2 (16443-1 AP, Proteintech), phosphorylated ERK1/2 (p-ERK1/2) (ab214362, Abcam), NF- κB p65 (10745-1 AP, Proteintech), phosphorylated NF- κB p65 (p-p65; ab86299, Abcam), and α -tubulin (112241-1 AP, Proteintech) were used.

Statistical Analysis

Statistically significant differences between groups were determined by the Student's *t* test. Differences with *P* values of less than .05 were considered statistically significant.

Results

STV-Na Protected N2a Cells Against Apoptosis Under Conditions of CoCl₂-Induced Hypoxia

The cell viability assays showed that CoCl₂ treatment decreased cell viability in a concentration- and time-dependent manners (Fig 1A and B). Compared with control, cell viability of N2a cells treated with 300 μM CoCl₂ for 24 hours significantly reduced to 52.8%. Therefore, a treatment of 300 μM CoCl₂ for 24 hours was used to induce N2a cell injury in subsequent experiments. As shown in Figure 1C, pretreatment with STV-Na progressively attenuated CoCl₂-induced cell injury in N2a cells and 20 μM STV-Na treatment had the most significant protective effect. Consistent with the results of cell viability assays, pretreatment with STV-Na notably suppressed CoCl₂-induced LDH release in N2a cells, which is a marker widely used to evaluate the damage and toxicity of cells,¹⁷ and 20 μM STV-Na treatment had the most significant effect (Fig 1D). Moreover, pretreatment with 20 μM STV-Na had the most significant effect on inhibiting CoCl₂-induced cell apoptosis, detected by flow cytometry (Fig 1E). Thus, we used 20 μM STV-Na in all subsequent experiments. Taken together, STV-Na protected N2a cells against CoCl₂-induced apoptosis.

STV-Na Attenuated the Upregulation of Intracellular Ca²⁺ Concentration in N2a cells Under Conditions of CoCl₂-Induced Hypoxia

Dysregulation of intracellular Ca²⁺ homeostasis has been reported to be a key mechanism on neuron apoptosis and plays a critical role in stroke.⁶ To investigate the effect of STV-Na on intracellular Ca²⁺ concentration in an in vitro ischemia model, Ca²⁺ expression was detected by Fluo-4 AM dye. As observed in Figure 2, compared with the control or STV-Na treatment alone group, the intracellular Ca²⁺ concentration in CoCl₂-treated N2a cells was significantly increased. As expected, pretreatment with STV-Na could effectively attenuate CoCl₂-induced upregulation of the intracellular Ca²⁺ concentration in N2a cells (Fig 2A and B).

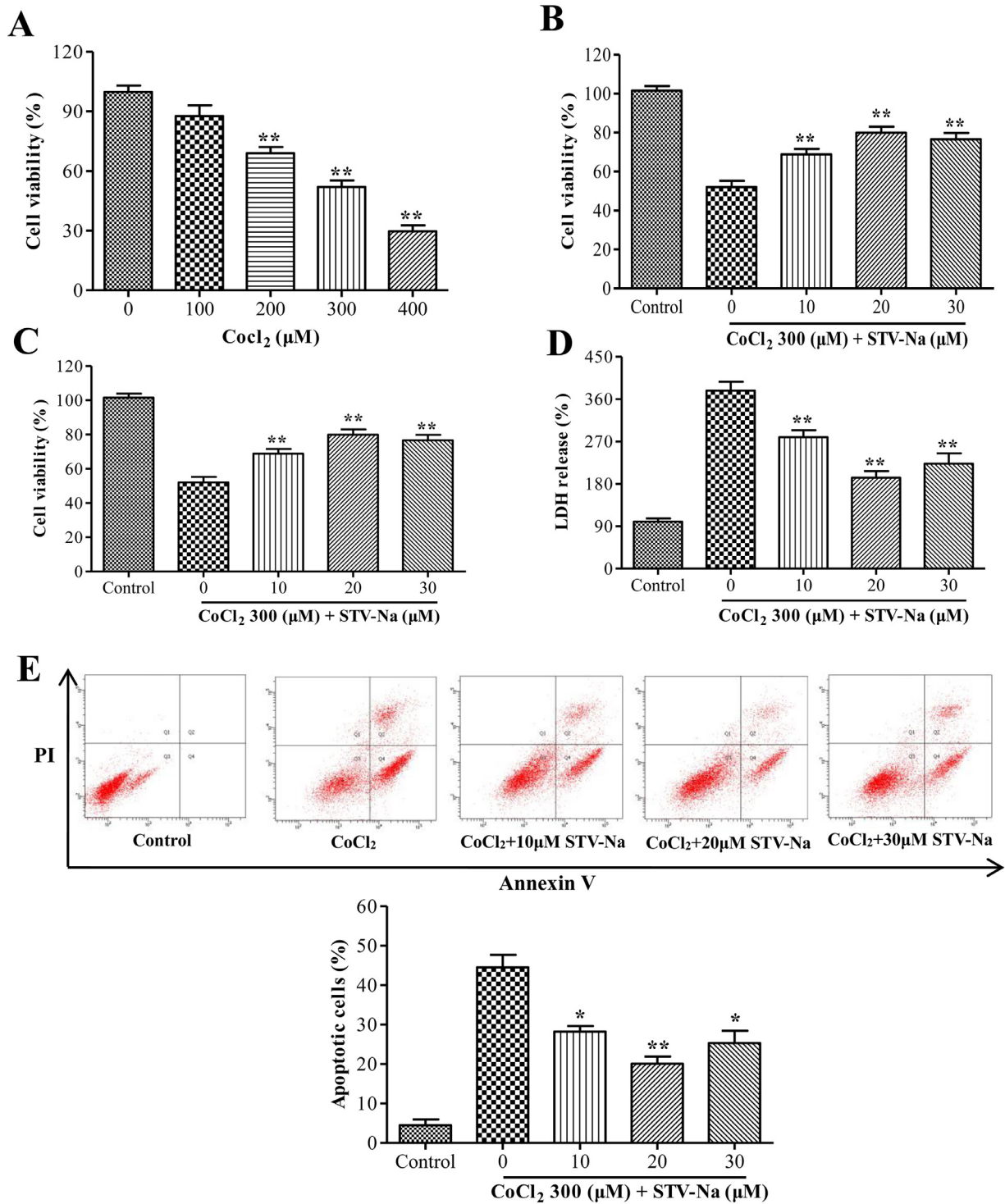


Figure 1. STV-Na protected N2a cells against apoptosis under conditions of CoCl₂-induced hypoxia. (A) N2a cells were treated with different concentrations of CoCl₂ for 24 hours. After that, cell viability was detected by CCK-8. (B) N2a cells were treated with 300 μM CoCl₂ for the indicated hours. After that, cell viability was detected by CCK-8. (C-E) N2a cells were pretreated with different concentrations of STV-Na 2 hours before exposure to 300 μM CoCl₂ treatment. After 24 hours, cell viability, LDH release and apoptotic rates were detected by CCK-8 (C), LDH Cytotoxicity Assay Kit (D) and flow cytometry (E), respectively. Data are represented as means ± SD (n = 3; *represents P < .05, **represents P < .01). Abbreviation: LDH, lactate dehydrogenase.

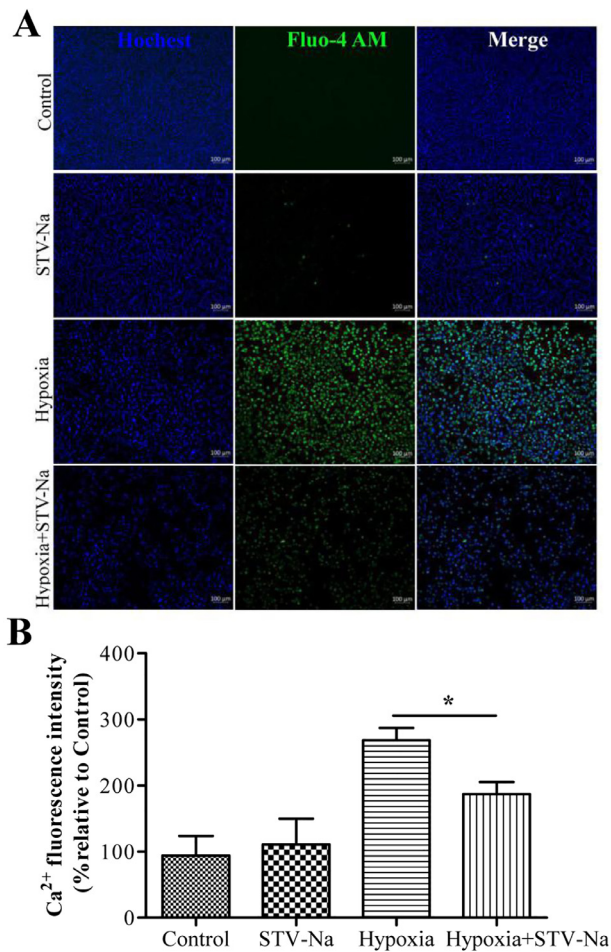


Figure 2. STV-Na attenuated the upregulation of intracellular Ca^{2+} concentration in N2a cells under conditions of CoCl_2 -induced hypoxia. (A) N2a cells were pretreated with $20 \mu\text{M}$ STV-Na 2 hours before exposure to $300 \mu\text{M}$ CoCl_2 treatment. After 24 h, the intracellular Ca^{2+} levels (green) were determined by Fluo-4 AM under fluorescence microscope. Nucleus were stained with Hoechst 33342 in blue. Control, normal N2a cells without any treatment; STV-Na, N2a cells treated with STV-Na, but not CoCl_2 ; Hypoxia, N2a cells treated with CoCl_2 ; Hypoxia + STV-Na, N2a cells treated with STV-Na before CoCl_2 treatment. (B) intracellular Ca^{2+} fluorescence intensity was measured and presented in bar graph. Data are represented as means \pm SD ($n = 3$; *represents $P < .05$, **represents $P < .01$). Abbreviation: SD, standard deviation. Color version of figure is available online.

STV-Na Relieved ROS Production, Mitochondrial Depolarization, and Proapoptotic Protein Expressions in N2a Cells Under Conditions of CoCl_2 -Induced Hypoxia

ROS overloaded and the depolarization of the mitochondrial membrane are the characteristic features of neuron apoptosis and are closely involved in the process of stroke.⁵ To investigate the effects of STV-Na pretreatment on the oxidative stress in N2a cells under conditions of CoCl_2 -induced hypoxia, we examined the ROS production and MMP using 2,7-Dichlorodi-hydrofluorescein diacetate (DCFH-DA) and JC-1 dye, respectively. As observed in Figure 3A and C, DCFH-DA fluorescence

intensity was significantly increased in N2a cells treated with CoCl_2 , compared with the control or STV-Na treatment alone group. However, STV-Na pretreatment markedly relieved ROS production in N2a cells under conditions of CoCl_2 -induced hypoxia. Similarly, STV-Na pretreatment significantly attenuated CoCl_2 -induced mitochondrial depolarization (Fig 3B and D), suggesting that STV-Na pretreatment suppressed oxidative stress responses in N2a cells under conditions of CoCl_2 -induced hypoxia.

To further understand the protective effects of STV-Na on mitochondrial function, we examined the expressions of Bax and Bcl2, which play important roles in regulating mitochondrial membrane potential integrity and maintaining mitochondrial function,^{5,28} in N2a cells under conditions of CoCl_2 -induced hypoxia. As shown in Figure 3E and F, hypoxia significantly induced an increase in the expression of proapoptotic protein Bax and cleaved Caspase3, and decrease in the expression of antiapoptotic protein Bcl-2, compared with the control or STV-Na treatment alone group. However, STV-Na pretreatment notably inhibited CoCl_2 -induced the upregulated expression of Bax and the downregulated expression of Bcl2, and decreased the Bax/Bcl2 expression ratio.

STV-Na Inhibited Proinflammatory Gene Expressions in N2a Cells Under Conditions of CoCl_2 -Induced Hypoxia

Proinflammatory cytokines such as $\text{TNF-}\alpha$, IL-6, IL-1 β , and iNOS play pivotal roles in neuron apoptosis and the pathogenesis of ischemic stroke. To investigate the effects of STV-Na treatment on the inflammatory response in N2a cells under conditions of CoCl_2 -induced hypoxia, we examined the mRNA expression levels of $\text{TNF-}\alpha$, IL-6, IL-1 β , and iNOS by qRT-PCR. The results showed that under conditions of CoCl_2 -induced hypoxia, the mRNA expression levels of $\text{TNF-}\alpha$, IL-6, IL-1 β , and iNOS were significantly elevated, compared with the control or STV-Na treatment alone group (Fig 4). When pretreated with STV-Na, $\text{TNF-}\alpha$, IL-6, IL-1 β , and iNOS mRNA expression levels were significantly inhibited in N2a cells under hypoxia condition, indicating that STV-Na could decrease inflammatory response after hypoxia injury.

STV-Na Inhibited MAPKs and NF- κB Signalings in N2a Cells Under Conditions of CoCl_2 -Induced Hypoxia

MAPKs and NF- κB signalings are activated in response to cerebral ischemia and play crucial roles in inducing proinflammatory mediators and apoptosis.¹³⁻¹⁶ Hence, we investigated whether MAPKs and NF- κB signalings participated in the neuroprotective effect of STV-Na on CoCl_2 -induced hypoxia injury by Western blotting. As shown in Figure 5, p-p38, p-ERK1/2, p-JNK, and p-p65 protein expression levels were all

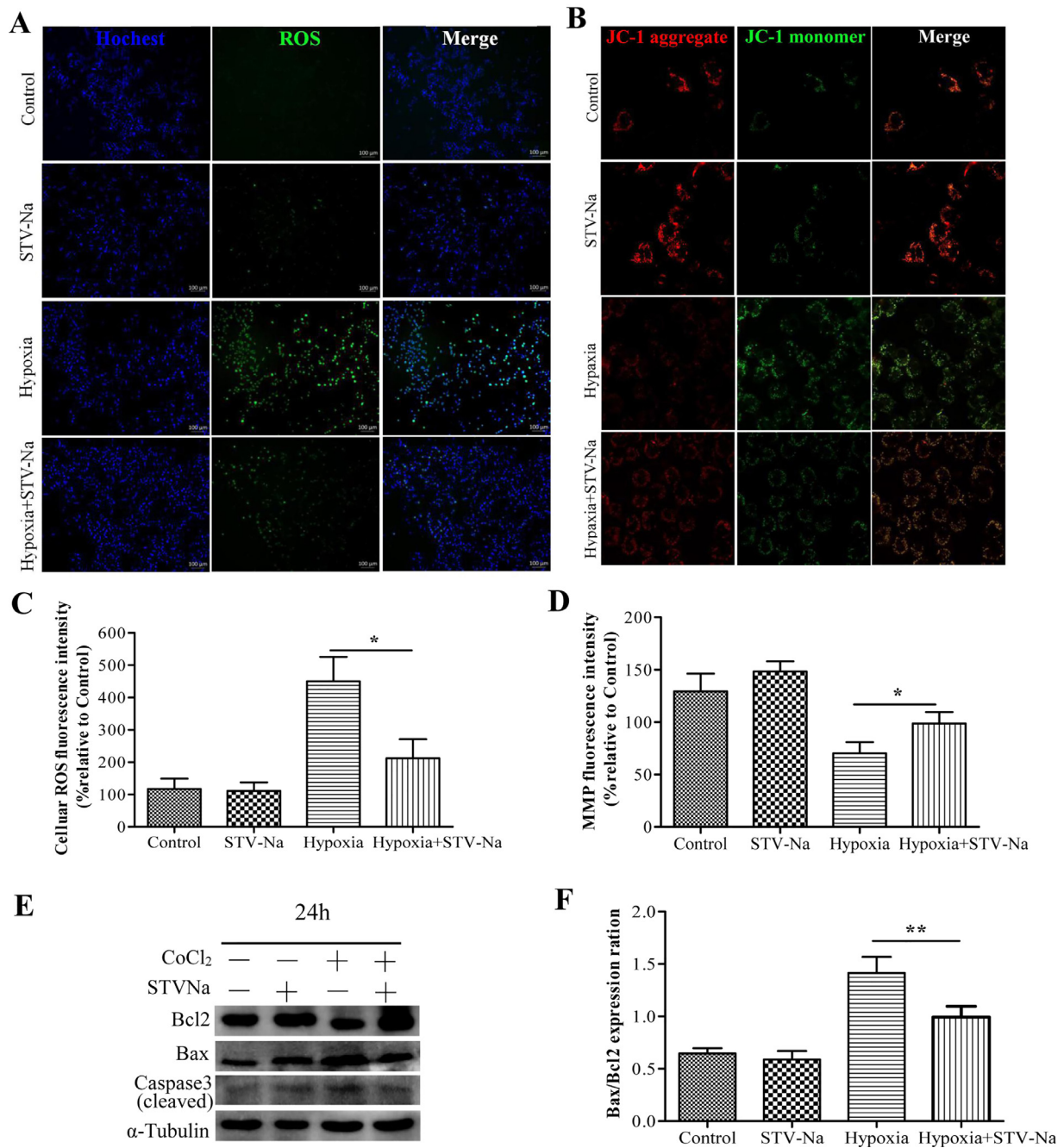


Figure 3. STV-Na relieved ROS production, mitochondrial depolarization, and proapoptotic protein expressions in N2a cells under conditions of CoCl₂-induced hypoxia. N2a cells were pretreated with 20 μ M STV-Na 2 hours before exposure to 300 μ M CoCl₂ treatment. After 24 hours, ROS production (A) and mitochondrial membrane potential (B) were determined by DCFH-DA or JC-1 dye, respectively. Nucleus were stained with Hoechst 33342 in blue. (C) ROS fluorescence intensity was measured and presented in bar graph. (D) MMP fluorescence intensity was calculated as the red/green fluorescence ratio. (E) Bax, Bcl2, cleaved caspase3, and α -tubulin protein expression levels were determined by Western blotting. (F) Bax/Bcl2 expression ratio was measured and presented in bar graph. Data are represented as means \pm SD ($n = 3$; *represents $P < .05$, **represents $P < .01$). Abbreviations: MMP, mitochondrial membrane potential; ROS, reactive oxygen species; SD, standard deviation. Color version of figure is available online.

significantly increased in N2a cells under conditions of CoCl₂-induced hypoxia, compared with the control or STV-Na treatment alone group. Whereas STV-Na pretreatment notably inhibited the CoCl₂-induced upregu-

lation expression of p-p38, p-ERK1/2, p-JNK, and p-p65 (Fig 5), suggesting that STV-Na protects neural cells against hypoxia-induced apoptosis through inhibiting MAPKs and NF- κ B pathways.

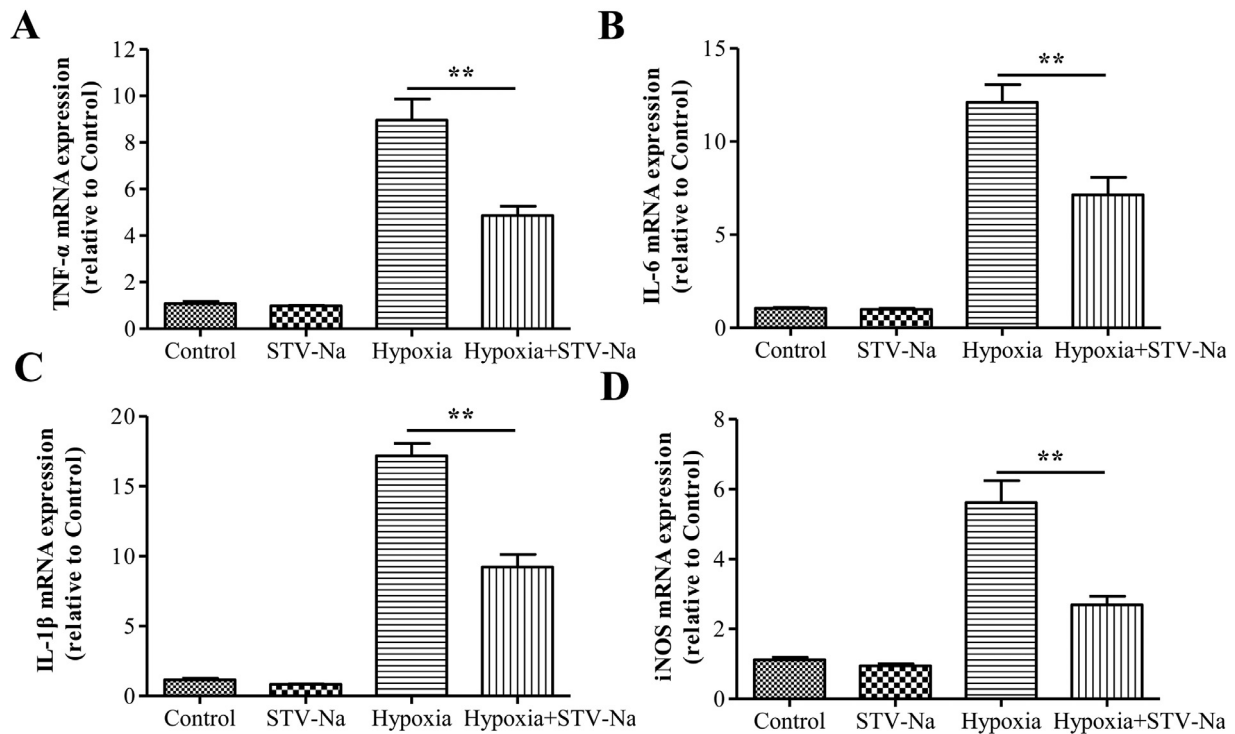


Figure 4. STV-Na inhibited proinflammatory gene expressions in N2a cells under conditions of CoCl_2 -induced hypoxia. N2a cells were pretreated with $20 \mu\text{M}$ STV-Na 2 hours before exposure to $300 \mu\text{M}$ CoCl_2 treatment. After 24 hours, mRNA expression levels of TNF- α (A), IL-6 (B), IL-1 β (C), and iNOS (D) were determined by qRT-PCR. Data are represented as means \pm SD ($n = 3$; *represents $P < .05$, **represents $P < .01$). Abbreviations: SD, standard deviation; qRT-PCR, quantitative real-time polymerase chain reaction.

Discussion

CoCl_2 -induced hypoxia injury model has been widely used to elucidate the mechanisms related to ischemia hypoxia-linked cell apoptosis in vitro in recent years,^{30,31} and STV-Na has been demonstrated to have neuroprotective effects on ischemia-induced injury.²⁴⁻²⁶ However, the potential mechanisms underlying the neuroprotective effect of STV-Na in hypoxia/ischemia-induced neuronal injury is still not known clearly. In the present study, we first demonstrate that STV-Na protects neural cells against hypoxia-induced apoptosis including attenuating the upregulation of intracellular Ca^{2+} concentration, ROS production, inhibiting mitochondrial depolarization in N2a cells under conditions of CoCl_2 -induced hypoxia through inhibiting MAPK and NF- κB pathways.

Accumulating evidence reveals that hypoxia/ischemia plays an extremely important role in secondary neuronal injury because this condition results in overloaded ROS.^{32,33} Excessive ROS production in the brain is widely believed to contribute to cerebral ischemia and neurodegenerative processes,³⁴ through inducing dysregulation of intracellular Ca^{2+} homeostasis and loss of MMP, eventually resulting in overexpressions of iNOS, IL-1 β , TNF- α , and IL-6. We observed that STV-Na protected the hypoxia-induced N2a from cell damage and significantly reduced ROS production following hypoxia (Fig 3A). Besides, STV-Na treatment significantly decreased the

loss of MMP and the expression of iNOS, IL-1 β , TNF- α , and IL-6 (Fig. 3 and 4).

The MAPK pathway contributes to the hypoxia-induced apoptosis in neuroblastoma cells.³⁵ Previous study demonstrated that hypoxia activated MAPK signaling pathways by enhancing phosphor-ERK, JNK, and p38 MAPKs in different cells.³⁶ STV-Na inhibited MAPKs cascades by inhibiting phosphor-ERK, JNK and p38 expression in N2a cells after 24 hours hypoxia (Fig 5). These observations are consistent with those reported by other investigators who stated that hypoxia resulted in the activation of MAPKs in neuronal cells^{32,37} and that inhibition of the phospho-JNK, ERK, or p38 MAPK pathways reduces acute ischemic injury.^{38,39} Other investigations have shown that inhibition of apoptotic markers (MAPKs and caspase-3) reduces hypoxia-induced neuron death.⁴⁰ Therefore, the effects of STV-Na might be mediated through repression of MAPK activation. Hypoxia-induced N2a cell death can be partially prevented by STV-Na. The effect of STV-Na on N2a cell death was probably via attenuation of ROS generation during hypoxia and the concomitant downregulation of MAPKs expression. Regulation of ROS generation, MAPK cascades, and apoptosis by STV-Na might lead to protection of neuronal cells from hypoxic insults.

NF- κB which is a family of transcription factors and known as a dominant regulator plays a critical role in inflammation, oxidative stress and immunity.⁴¹ NF- κB signaling

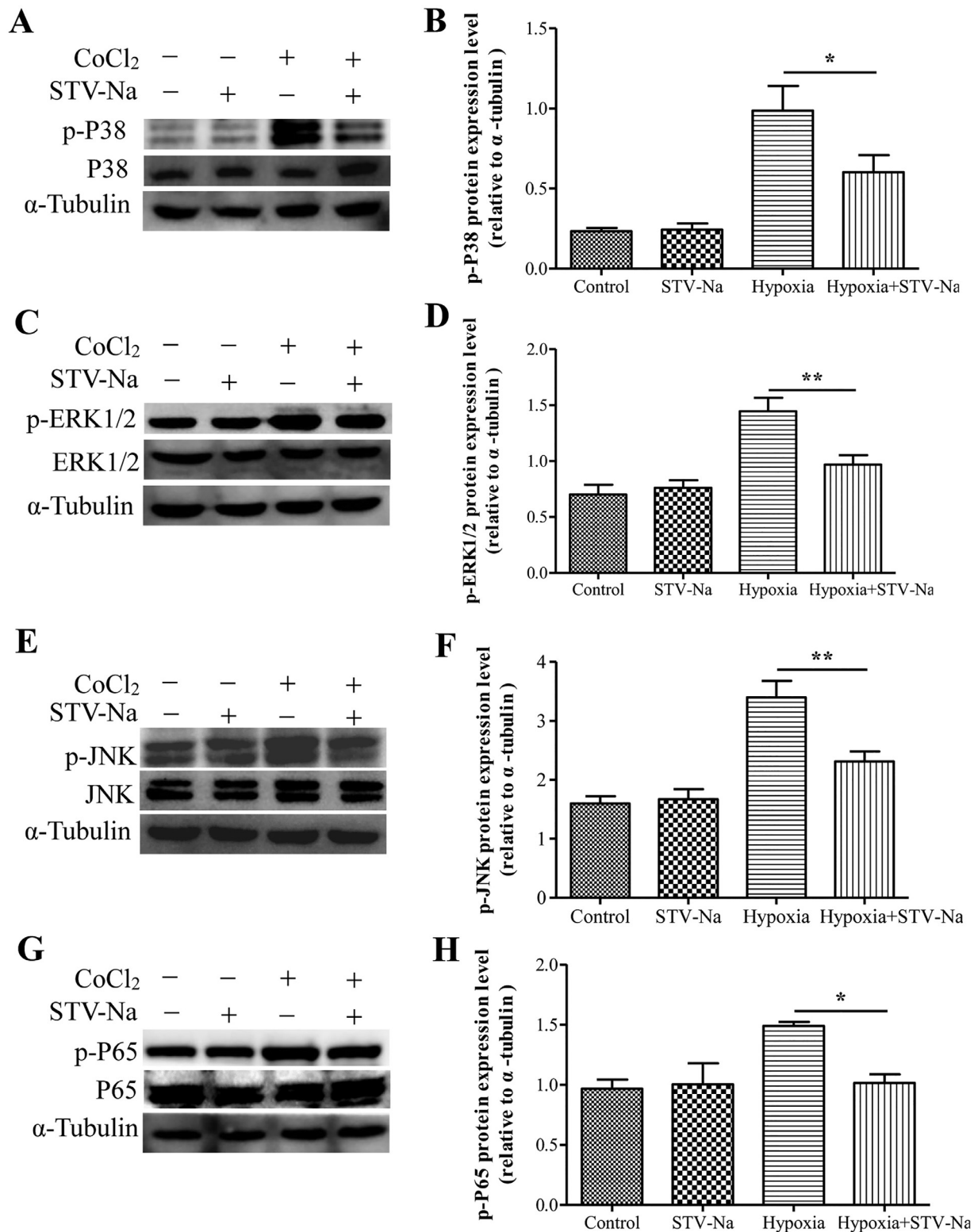


Figure 5. STV-Na inhibited MAPKs and NF- κ B signalings in N2a cells under conditions of CoCl₂-induced hypoxia. N2a cells were pretreated with 20 μ M STV-Na 2 hours before exposure to 300 μ M CoCl₂ treatment. After 24 hours, protein expression levels of α -tubulin, p38, p-p38 (A), ERK1/2, p-ERK1/2 (C), JNK, p-JNK (E), p65, p-p65 (G) were determined by Western blotting. Relative expression level of p-p38 (B), p-ERK1/2 (D), p-JNK (F), and p-p65 (H) were calculated by normalizing to that of α -tubulin, respectively. Data are represented as means \pm SD (n = 3; *represents P < .05, **represents P < .01). Abbreviations: MAPK, mitogen-activated protein kinase; SD, standard deviation.

pathway could be activated or inactivated by different factors or stimulus signaling, such as TNF- α , caspase-3, JNK, ROS, and ERK.⁴² On the contrary, upon stimulation, the activation of NF- κ B could induce the expression of many proinflammatory genes, including COX-2, TNF- α , and iNOS.⁴³ Meanwhile, the activation of NF- κ B signaling pathway can regulate apoptosis under the hypoxic environment.⁴⁴ The previous study showed that STV-Na could protect against permanent cerebral ischemia and experimental traumatic brain injury via Inhibition of NF- κ B-mediated inflammatory and apoptotic responses. Consistently, in the present study, STV-Na treatment could significantly reduce the expressions of p-P65 protein and its downstream TNF- α , IL-6, IL-1 β , and iNOS mRNA expression levels were significantly inhibited (Fig 4). Thus, we hypothesized that STV-Na may have a neuroprotective effect through inhibition of NF- κ B signaling pathway to attenuate apoptosis by hypoxia.

In some diseases of ischemia and hypoxia, abnormal pathological reaction enhances the MAPK or NF- κ B signaling pathway.⁴¹ The aberrant activations of MAPK and NF- κ B signaling pathways both have critical effects on hypoxia-induced apoptosis and death,^{36–39} which was found in N2a cells according to previous studies.³⁶ According to our reports, we observed that STV-Na pretreatment suppressed hypoxia-caused upregulation of the phosphorylation activity of ERK, JNK, p38, and NF- κ B-p65. This indicated that STV-Na might mediate the hypoxia progression in N2a cells by inhibiting cellular apoptosis, which was linked to MAPK and NF- κ B signaling pathways. In conclusion, this study provided the novel mechanistic evidence that STV-Na attenuates the CoCl₂-induced apoptosis and cytotoxicity through inhibition of the MAPK and NF- κ B pathway in N2a cells. The findings of this study provide the clues for STV-Na treatment to cerebral ischemia, such as anti-inflammation, anticytotoxicity, antiapoptosis, antioxidative stress, antiendoplasmic stress, and mitochondrial protection. However, more studies are required, such as animal experiment in vivo and the effects of STV-Na on CoCl₂-treated different cells or organs.

Conflict of Interest

The authors have no conflicts of interest to disclose.

Acknowledgments: The authors are grateful to Key Pharmaceutical Co. Ltd. for supplying STV-Na.

References

1. Krishnamurthi RV, deVeber G, Feigin VL, et al. Stroke prevalence, mortality and disability-adjusted life years in children and youth aged 0-19 years: data from the global and regional burden of stroke 2013. *Neuroepidemiology* 2015;45:177-189.
2. Lees KR, Bluhmki E, von Kummer R, et al. Time to treatment with intravenous alteplase and outcome in stroke: an updated pooled analysis of ECASS, ATLANTIS, NINDS, and EPITHET trials. *Lancet* 2010;375:1695-1703.
3. Downie S. Quality improvement in acute stroke: the New York State Stroke Center Designation Project. *Neurology* 2007;68:965. author reply.
4. Dirnagl U, Iadecola C, Moskowitz MA. Pathobiology of ischaemic stroke: an integrated view. *Trends Neurosci* 1999;22:391-397.
5. Huttemann M, Helling S, Sanderson TH, et al. Regulation of mitochondrial respiration and apoptosis through cell signaling: cytochrome c oxidase and cytochrome c in ischemia/reperfusion injury and inflammation. *Biochim Biophys Acta* 2012;1817:598-609.
6. Depp C, Bas-Orth C, Schroeder L, Hellwig A, et al. Synaptic activity protects neurons against calcium-mediated oxidation and contraction of mitochondria during excitotoxicity. *Antioxid Redox Signaling* 2017.
7. Abouzaki NA, Christopher S, Trankle C, et al. Inhibiting the inflammatory injury following myocardial ischemia reperfusion with plasma derived alpha-1 anti-trypsin: a post-hoc analysis of the VCU-alpha1RT study. *J Cardiovasc Pharmacol* 2018.
8. Anuncibay-Soto B, Perez-Rodriguez D, Santos-Galdiano M, et al. Salubrinal and robenacoxib treatment after global cerebral ischemia. Exploring the interactions between ER stress and inflammation. *Biochem Pharmacol* 2018;151:26-37.
9. Qu Y, Zhang HL, Zhang XP, et al. Arachidonic acid attenuates brain damage in a rat model of ischemia/reperfusion by inhibiting inflammatory response and oxidative stress. *Hum Exp Toxicol* 2018;37:135-141.
10. Iadecola C, Anrather J. The immunology of stroke: from mechanisms to translation. *Nat Med* 2011;17:796-808.
11. Dong HJ, Shang CZ, Peng DW, et al. Curcumin attenuates ischemia-like injury induced IL-1beta elevation in brain microvascular endothelial cells via inhibiting MAPK pathways and nuclear factor-kappaB activation. *Neurol Sci Off J Ital Neurol Soc Ital Soc Clin Neurophysiol* 2014;35:1387-1392.
12. Gu J, Su S, Guo J, et al. Anti-inflammatory and anti-apoptotic effects of the combination of Ligusticum chuanxiong and Radix Paeoniae against focal cerebral ischaemia via TLR4/MyD88/MAPK/NF-kappaB signaling pathway in MCAO rats. *J Pharm Pharmacol* 2018;70:268-277.
13. Lin Y, Liu Q, Chen C, et al. [Effect of acupuncture combined with hypothermia on MAPK/ERK pathway and apoptosis related factors in rats with cerebral ischemia reperfusion injury]. *Zhong nan da xue xue bao Yi xue ban J Cent South Univ Med Sci* 2017;42:380-388.
14. Song YS, Lee YS, Narasimhan P, et al. Reduced oxidative stress promotes NF-kappaB-mediated neuroprotective gene expression after transient focal cerebral ischemia: lymphocytotropic cytokines and antiapoptotic factors. *J Cereb Blood Flow Metab Off J Int Soc Cereb Blood Flow Metab* 2007;27:764-775.
15. Song YS, Narasimhan P, Kim GS, et al. The role of Akt signaling in oxidative stress mediates NF-kappaB activation in mild transient focal cerebral ischemia. *J Cereb Blood Flow Metab Off J Int Soc Cereb Blood Flow Metab* 2008;28:1917-1926.

16. Gu N, Ge K, Hao C, et al. Neuregulin1beta effects on brain tissue via ERK5-Dependent MAPK pathway in a rat model of cerebral ischemia-reperfusion injury. *J Mol Neurosci* 2017;61:607-616.
17. Ma LL, Xing GP, Yu Y, et al. Sulforaphane exerts neuroprotective effects via suppression of the inflammatory response in a rat model of focal cerebral ischemia. *Int J Clin Exp Med* 2015;8:17811-17817.
18. Ahmed MA, El Morsy EM, Ahmed AA. Pomegranate extract protects against cerebral ischemia/reperfusion injury and preserves brain DNA integrity in rats. *Life Sci* 2014;110:61-69.
19. Li G, Tian Y, Zhang Y, et al. A novel ligustrazine derivative T-VA prevents neurotoxicity in differentiated PC12 Cells and protects the brain against ischemia injury in MCAO Rats. *Int J Mol Sci* 2015;16:21759-21774.
20. Jeppesen PB, Gregersen S, Rolfsen SE, et al. Antihyperglycemic and blood pressure-reducing effects of stevioside in the diabetic Goto-Kakizaki rat. *Metabolism* 2003;52:372-378.
21. Liu JC, Kao PK, Chan P, et al. Mechanism of the antihypertensive effect of stevioside in anesthetized dogs. *Pharmacology* 2003;67:14-20.
22. Takasaki M, Konoshima T, Kozuka M, et al. Cancer preventive agents. Part 8: chemopreventive effects of stevioside and related compounds. *Bioorganic & medicinal chemistry* 2009;17:600-605.
23. Lai W, Kang Q, Zou C, et al. Development of a liquid formulation of poorly water-soluble isosteviol sodium using the co-solvent technology. *Pharm Dev Technol* 2017;22:275-282.
24. Zhang H, Sun X, Xie Y, et al. Isosteviol Sodium Protects Against Permanent Cerebral Ischemia Injury in Mice via Inhibition of NF- κ B—Mediated Inflammatory and Apoptotic Responses. *J Stroke Cerebrovasc Dis* 2017;26(11):2603-2614.
25. Zan J, Zhang H, Lu MY, et al. Isosteviol sodium injection improves outcomes by modulating TLRs/NF- κ B-dependent inflammatory responses following experimental traumatic brain injury in rats. *Neuroreport* 2018;29(10):1.
26. Zhang H, Sun X, Xie Y, et al. Isosteviol sodium inhibits astrogliosis after cerebral ischemia/reperfusion injury in rats. *Biol Pharm Bull* 2018;41(4):575-584.
27. Chen R, Xu J, She Y, et al. Necrostatin-1 protects C2C12 myotubes from CoCl₂-induced hypoxia. *Int J Mol Med* 2018;41:2565-2572.
28. Hu J, Zhao TZ, Chu WH, et al. Protective effects of 20-hydroxyecdysone on CoCl₂-induced cell injury in PC12 cells. *J Cell Biochem* 2010;111:1512-1521.
29. Nieswandt B, Kleinschnitz C, Stoll G. Ischaemic stroke: a thrombo-inflammatory disease? *J Physiol* 2011;589:4115-4123.
30. Meng JL, Mei WY, Dong YF, et al. Heat shock protein 90 mediates cytoprotection by H₂S against chemical hypoxia-induced injury in PC12 cells. *Clin Exp Pharmacol Physiol* 2011;38:42-49.
31. Zou W, Zeng J, Zhuo M, et al. Involvement of caspase-3 and p38 mitogen-activated protein kinase in cobalt chloride-induced apoptosis in PC12 cells. *J Neurosci Res* 2002;67:837-843.
32. Hou CW, Huang HM, Tzen JTC, et al. Protective effects of sesamin and sesamol on hypoxic neuronal and PC12 cells. *J Neurosci Res* 2003;74:123.
33. Hwang SL, Yen GC. Neuroprotective effects of the citrus flavanones against H₂O₂-induced cytotoxicity in PC12 cells. *J Agric Food Chem* 2008;56:859.
34. Lobysheva NV, Tonshin AA, Selin AA, et al. Diversity of neurodegenerative processes in the model of brain cortex tissue ischemia. *Neurochem Int* 2009;54:322-329.
35. Cao M, Jiang J, Yifeng DU, et al. Mitochondria-targeted antioxidant attenuates high glucose-induced P38 MAPK pathway activation in human neuroblastoma cells. *Mol Med Report* 2012;5:929-934.
36. Hu J, Li T, Du S, et al. The MAPK signaling pathway mediates the GPR91-dependent release of VEGF from RGC-5 cells. *Int J Mol Med* 2015;36:130-138.
37. Lennon AM, Ramaugé M, Dessouroux A, et al. MAP kinase cascades are activated in astrocytes and preadipocytes by 15-deoxy-Delta(12-14)-prostaglandin J(2) and the thiazolidinedione ciglitazone through peroxisome proliferator activator receptor gamma-independent mechanisms involving reactive oxygenate. *J Biol Chem* 2002;277:29681-29685.
38. Legos JJ, Mclaughlin BA, Skaper SD, et al. The selective p38 inhibitor SB-239063 protects primary neurons from mild to moderate excitotoxic injury. *Eur J Pharmacol* 2002;447:37-42.
39. Chen J, Guo R, Yan H, et al. Naringin inhibits ROS-activated MAPK pathway in high glucose-induced injuries in H9c2 cardiac cells. *Basic Clin Pharmacol Toxicol* 2014;114:293-304.
40. Tabakman R, Jiang H, Levine RA, Kohen R, Lazarovici P. Apoptotic characteristics of cell death and the neuroprotective effect of homocarnosine on pheochromocytoma PC12 cells exposed to ischemia. *J Neurosci Res* 2004;75:499.
41. Hoesel B, Schmid JA. The complexity of NF- κ B signaling in inflammation and cancer. *Mol Cancer* 2013;12:86.
42. Jiang ZY, Guo YY, Ren HB, et al. Tumor necrosis factor (TNF)- α upregulates progesterone receptor-A by activating the NF- κ B signaling pathway in human decidua after labor onset. *Placenta* 2012;33:1-7.
43. Cheng G., Zhao Y., Li H., et al. Forsythiaside attenuates lipopolysaccharide-induced inflammatory responses in the bursa of Fabricius of chickens by downregulating the NF- κ B signaling pathway. 2014;7:179-184.
44. Sun ZJ, Gang C, Xiang H, et al. Activation of PI3K/Akt/IKK- α /NF- κ B signaling pathway is required for the apoptosis-evasion in human salivary adenoid cystic carcinoma: its inhibition by quercetin. *Apoptosis* 2010;15:850-863.